Monthly Notices
of the
ROYAL ASTRONOMICAL SOCIETY

MNRAS **450,** 3840–3854 (2015) doi:10.1093/mnras/stv687

Missing hard states and regular outbursts: the puzzling case of the black hole candidate 4U 1630–472

F. Capitanio,[1⋆] R. Campana,[2] G. De Cesare[2] and C. Ferrigno[3]

[1]*INAF–IAPS, Via Fosso del Cavaliere, 100, I-00133 Roma, Italy*
[2]*INAF–IASF, Via Piero Gobetti, 101, I-40129 Bologna, Italy*
[3]*INTEGRAL Science Data Centre for Astrophysics, Chemin d'Ecogia 16, CH-1290 Versoix, Switzerland*

Accepted 2015 March 25. Received 2015 March 20; in original form 2014 August 10

ABSTRACT

4U 1630–472 is a recurrent X-ray transient classified as a black hole candidate from its spectral and timing properties. One of the peculiarities of this source is the presence of regular outbursts with a recurrence period between 600 and 730 d that has been observed since the discovery of the source in 1969. We report on a comparative study of the spectral and timing behaviour of three consecutive outbursts that occurred in 2006, 2008 and 2010. We have analysed all the data collected by *INTEGRAL* and the *Rossi X-ray Timing Explorer* (*RXTE*) during these three years of activity. We show that, in spite of having a similar spectral and timing behaviour in the energy range between 3 and 30 keV, these three outbursts show pronounced differences above 30 keV. In fact, the 2010 outburst extends at high energies without any detectable cut-off until 150–200 keV, while the two previous outbursts that occurred in 2006 and 2008 are not detected at all above 30 keV. Thus, in spite of a very similar accretion disc evolution, these three outbursts exhibit totally different characteristics of the Compton electron corona, showing a softening in their evolution rarely observed before in a low-mass X-ray binary hosting a black hole. We argue the possibility that the unknown perturbation that causes the outbursts to be equally spaced in time could be at the origin of this particular behaviour. Finally, we describe several possible scenarios that could explain the regularity of the outbursts, identifying the most plausible, such as a third body orbiting around the binary system.

Key words: black hole physics – methods: data analysis – binaries: close – stars: black holes – X-rays: binaries – X-rays: individual: 4U1630-472.

1 INTRODUCTION

4U 1630–472 is one of the most active black hole candidates (BHCs) ever observed. The first known outburst was detected by the *Vela 5B* satellite in 1969 (Priedhorsky 1986). Since then, the source has undergone an outburst at least 20 times, and has been observed by most of the principal X-ray missions, which have collected a huge amount of data.

4U 1630–472 is a highly absorbed source with a hydrogen column density that varies in the range of $N_{\rm H} = (4–12) \times 10^{22}$ cm^{-2} (Kuulkers et al. 1998; Tomsick, Lapshov & Kaaret 1998). The distance and the mass of the compact object have still not been firmly measured because no optical counterpart has been identified up to now. This is mostly due to the crowded region in which the source lies. Thus, 4U 1630–472 is still classified as a BHC because of its characteristic spectral and timing behaviour.

Seifina, Titarchuk & Shaposhnikov (2014) have recently reported an indirect estimation of the mass (10 $M_\odot$) on the basis of the detection of the spectral index saturation with the mass accretion rate (see also Shaposhnikov & Titarchuk 2009). The infrared (IR) counterpart was instead detected during the 1998 outburst, as reported by Augusteijn, Kuulkers & van Kerkwijk (2001). The analysis of the IR photometric data reveals that 4U 1630–472 is a highly reddened source lying in the direction of a giant molecular cloud that is located at a distance of 11 kpc. 4U 1630–472 lies in the near side of this cloud, thus at a distance <11 kpc. However, the high absorption indicates a large distance, >10 kpc (Seifina et al. 2014). Thus, it is reasonable to assume a source distance of ∼10–11 kpc. The IR properties are consistent with a relatively long orbital period system ($P_{\rm orb} \sim$ a few days) containing an early-type secondary star. Anyway, the range in absolute *K*-band magnitude and the observed IR variability cannot exclude a B star nature (intrinsically slightly reddened) in a detached Be/X-ray binary (Augusteijn et al. 2001).

Dieters et al. (2000) and Trudolyubov, Borozdin & Priedhorsky (2001) report on detailed X-ray spectral and timing analysis of the 1998 outburst of 4U 1630–472. They show that the source behaviour is typical of a BHC. During the same outburst, the detection of a polarized radio emission revealed the presence of optically thin radio jets ejected from the source (Hjellming et al. 1999).

⋆ E-mail: fiamma.capitanio@iaps.inaf.it

Several radio observation campaigns have been carried out during the subsequent outbursts. Nevertheless, most of them failed to detect any radio emission from the source (Hannikainen et al. 2002; Gallo et al. 2006; Calvelo et al. 2010).

Tomsick et al. (1998) report the detection of a dip in the *Rossi X-ray Timing Explorer* (*RXTE*) Proportional Counter Array (PCA) data during the 1996 observations. This implies that the inclination angle is probably greater than 60°. *Suzaku* X-ray satellite observations in 2006 revealed significant absorption lines from highly ionized iron lines with a blueshift that corresponds to an outflow velocity of about 1000 km s^{-1} (Kubota et al. 2007). This fact supports the hypothesis that the source is viewed at a high inclination angle (Ponti, Fender & Begelman 2012), even though, after 1996, no more dips have been reported in the literature. The scaling technique (see Shaposhnikov & Titarchuk 2009, and references therein) permits Seifina et al. (2014) to constrain the inclination angle of the system at $i \leq 70°$.

Díaz Trigo et al. (2013) report on the detection of Doppler-shifted X-ray emission lines in coincidence with the reappearance of radio emission from the jets during the 2012 outburst. They argue that these lines arise from baryonic matter in a relativistic jet. However, Neilsen et al. (2014) show that the radio emission during the same outburst was not always associated with relativistic emission lines, and the unique behaviour reported by Díaz Trigo et al. (2013) might be a special case, dependent on additional processes in the accretion flow around the black hole (BH).

King et al. (2014) report the clear detection of a reflection component in a short observation performed with the *NuSTAR* telescope during the 2013 outburst, when the source was in an intermediate state. The consequent spin measurement indicates that 4U 1630–472 harbours a rapidly spinning BH.

A unique characteristic of 4U 1630–472 is that the outbursts that have been observed from the first detection in 1969 have been roughly equally spaced in time, with a period of about 600 d (Parmar, Angelini & White 1995). As the 4U 1630–472 long-term *RXTE*/PCA light curve shows (Fig. 1, top panel), the recurrence is still present after more than 40 yr, even though a drift in the recurrence period of about 130 d has been observed in the last three outbursts, 2008–2012 (Capitanio et al. 2010). A similar drift in the recurrence period between one outburst and a subsequent outburst was previously noticed by Kuulkers et al. (1997). In addition, 4U 1630–472 is known to show peculiar outbursts that often lack bright hard states (for example, see Abe et al. 2005; Tomsick et al. 2014, and references therein).

The aim of this paper is to perform a comparative study of the high-energy behaviour of three consecutive outbursts of 4U 1630–472 that occurred between 2006 and 2010. In Section 2, we introduce the data collection criteria, the data reduction methods and the techniques employed for the spectral and timing analysis. In Section 3, we describe the general behaviour of the source during the three outbursts. In Section 4, we discuss the implication of the peculiar behaviour of the three outbursts in light of the standard theory of accretion flow on to a low-mass X-ray binary (LMXRB) hosting a BH. In the same section we describe the possible scenarios that could also explain the periodic recurrence of the outbursts. Finally, we summarize our findings and conclusions in Section 5.

2 DATA REDUCTION AND ANALYSIS

The 2008–2010 outbursts of 4U 1630–472 were extensively observed by the *RXTE* and *INTEGRAL* satellites. More than 800 ks of observations have been collected by the *RXTE* PCA, while 850 ks have been collected by the *INTEGRAL* γ-ray telescope IBIS (Ubertini et al. 2003).

The *RXTE*/PCA observation campaign covered the period of the three outbursts from MJD 53727 to MJD 55459 for a total of 441 pointings. The PCA analysis was performed with the standard *RXTE* software within HEASOFT 12.7.1 following the standard extraction procedure for light curves and spectra. For the PCA spectral analysis, a systematic error of 0.6 per cent (Wilms et al. 2006) was added

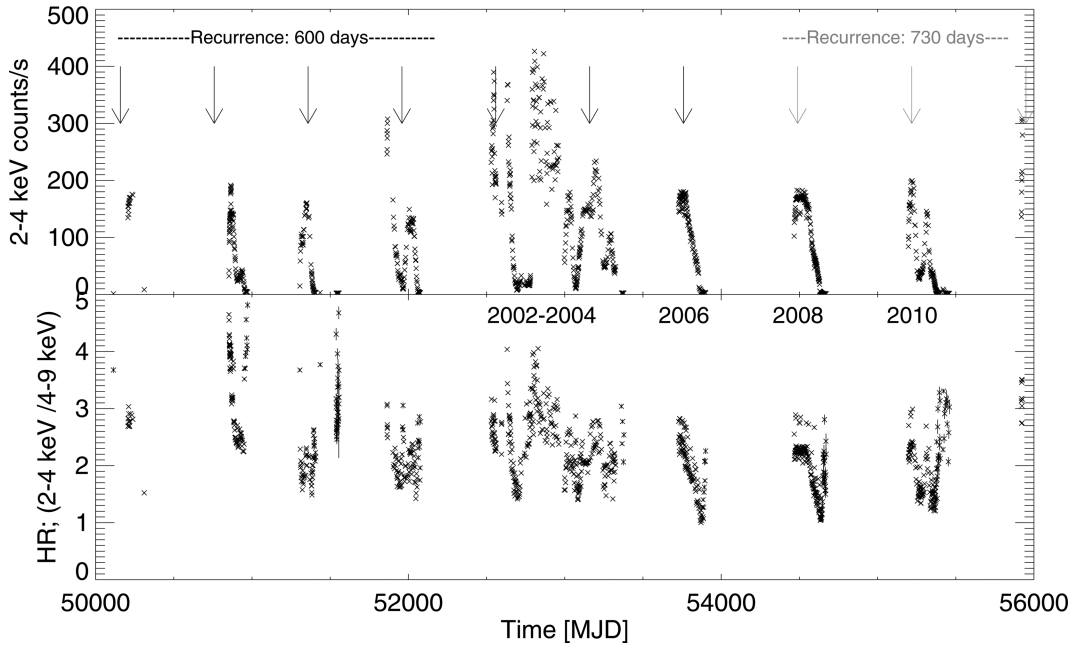

Figure 1. Top panel: 2–4 keV PCA long-term light curve of 4U 1630–472. Each point corresponds to a single PCA observation. Bottom panel: HR (4–9 keV/2–4 keV) versus time as observed by *RXTE*/PCA during all of its observational life (1996–2011). The black and grey arrows show the 600-d and 730-d recurrence periods of the outbursts, respectively (see Section 1 for details).

to the spectra. For the fitting procedure, the energy range 3–30 keV was used.

The timing analysis of the PCA was performed with custom software: for each of the observations, we produced power spectra from 16-s stretches accumulated in the channel band 0–35 (2–15 keV) with a time resolution of 1/125 s. The resulting power spectra were then averaged in one power spectrum per observation, normalized according to Leahy et al. (1983) and then converted into squared fractional rms (Belloni & Hasinger 1990; Miyamoto et al. 1991). The contribution due to Poissonian statistics was subtracted as reported by Zhang et al. (1995).

For the *INTEGRAL* data analysis, we used the latest release of the standard Offline Scientific Analysis (OSA, version 10.0), distributed by the *INTEGRAL* Science Data Centre (ISDC; Courvoisier et al. 2003). The *INTEGRAL* analysis was focused on the low-energy detector (ISGRI; Lebrun et al. 2003) of the γ-ray telescope IBIS. The ISGRI spectra were extracted in the 20–200 keV energy range. A systematic error of 2 per cent was taken into account for spectral analysis (see also Jourdain et al. 2008). In order to collect enough counts in a single spectrum, we added together contiguous IBIS spectra showing the same shape. We obtained 13 IBIS spectra, each of which was quasi-simultaneous with a single PCA observation.

The faintness of the source in most of the data and the limited energy range (3–30 keV) allowed us to model the 441 PCA spectra of the three outbursts only with a simple model, that is, an absorbed multicolour disc blackbody (Sakura & Sunyaev 1973) plus a power law to model the Comptonization of soft photons in a hot plasma: WABS×(DISKBB+POW), hereafter Model 1. We also attempted to model the Comptonization, instead of the power law, with two different simple physical models, NTHCOMP (Zdziarski, Johnson & Magdziarz 2004) or COMPTT (Titarchuk 1994): WABS*(DISKBB+NTHCOMP) and WABS*(DISKBB+COMPTT), hereafter Models 2 and 3, respectively. Because the cut-off is not constrained by the data, we do not succeed in constraining the plasma temperature. Thus, we fixed the electron plasma temperature at 15 keV for the 2006 and 2008 outburst spectra, and at 100 keV for the 2010 spectra (see Sections 3.1, 3.2 and 3.3 for details). The temperature of the seed photons was, instead, fixed at the same value of the multicolour disc blackbody model for Model 2, while for Model 3, the seed photon temperature was fixed for each observation at its best-fitting value. The statistics, the energy range and the resolution of the spectra did not allow us to apply any other more refined models.

Because of the limited PCA low-energy coverage, the equivalent hydrogen column, $N_{\rm H}$, was allowed to vary between a range of values extracted from the different results reported in the literature, (4–12) $\times$ 10^{22} cm^{-2} (e.g. Trudolyubov et al. 2001; Tomsick et al. 2005).

In order to improve the fit, we added a Gaussian component to the model in some of the observations, especially the ones where the source is particularly faint. This is not only due to an intrinsic Fe emission line but also due to the Galactic ridge emission-line contribution not completely corrected in the PCA data and to a nearby source, IGR J16320–4751, which has a prominent iron emission line (see Section 2.1 for details). The χ^2 statistic was used to determine the goodness of the fit. Only 4 per cent of the PCA pointings were immediately excluded because of an unacceptable χ^2/degree of freedom (d.o.f.), 10 per cent in the case of the Comptonization models. The excluded data mostly belong to the last part of the three outbursts when the source is very faint and the contamination due to the nearby source can no longer be neglected (see Section 2.1 for details). Thus, the accepted data have $\bar{\chi}^2_{\rm red} = 1.0$ with a maximum spread of $0.5 < \chi^2_{\rm red} < 1.9$, and with 76 per cent of the values that lie in the range, $0.8 < \chi^2_{\rm red} < 1.2$. Fig. 2 shows the distribution of the $\chi^2_{\rm red}$ values of the accepted PCA data. All the errors and upper limits reported in the paper correspond to the 90 per cent confidence level.

A normalization constant was added to the data model used to fit the 13 PCA–IBIS joint spectra to consider the calibration of the two different instruments. Moreover, because of their broad-band (3–200 keV), they were also modelled taking into account more refined models.

First, we applied a more refined Comptonization model such as COMPPS (Poutanen & Svensson 1996) in order to model the high-energy part of the joint PCA–IBIS spectra. However, any attempt to discriminate between thermal, non-thermal or hybrid Comptonization did not succeed in constraining the parameters (see Section 3.3 for details).

Then, we considered the possible presence of a reflection component (Ross & Fabian 2007). The model used was an absorbed multicolour disc blackbody (Sakura & Sunyaev 1973) plus a reflected power law in a neutral medium (Magdziarz & Zdziarski 1995, PEXRAV) that leads to a rapid computation (Fabian & Ross 2010): WABS*(DISKBB+PEXRAV), hereafter Model 4. Because the PCA–IBIS joint spectra do not show any cut-off, the PEXRAV parameter linked to the energy cut-off was fixed to zero as required by the model.

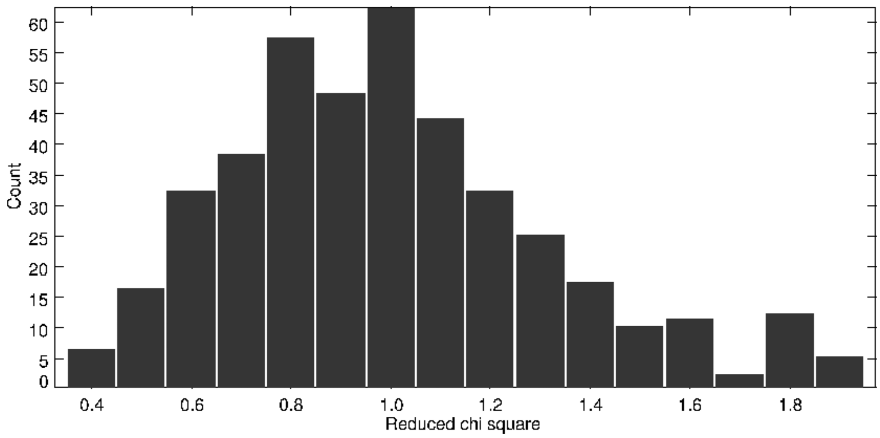

Figure 2. Distribution of the reduced χ^2 values of the accepted PCA data fit.

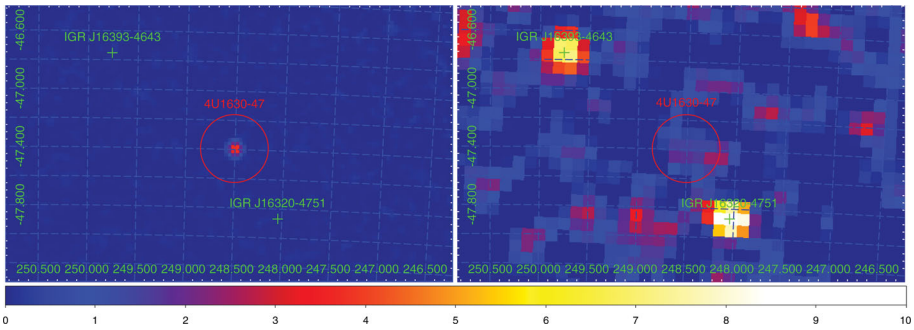

Figure 3. Left panel: 3–7 keV 2006 outburst JEM-X mosaic image of 4U 1630–472 and IGR J16320–4751 sky field (exposure 14 ks for a total of six science windows that belong to revolutions 399, 407, 411, 419, 423; MJD interval is 53756–53826). Right panel: 20–40 keV 2006 outburst IBIS mosaic image of 4U 1630–472 and IGR J16320–4751 sky field (exposure 31 ks for a total of 14 science windows that span from revolution 399 until revolution 427; MJD interval is 53756–53840).

2.1 Contamination of the *RXTE* data by a nearby source, IGR J16320–4751

The PCA collimated field of view (FOV) has a radius of 1°. Thus, as also reported by Tomsick et al. (2014), the PCA data of 4U 1630–472 could be contaminated by the nearby persistent X-ray source IGR J16320–4751, which is a well-studied high-mass X-ray binary (HMXRB) discovered by *INTEGRAL* in 2003 (e.g. Rodriguez et al. 2006) and lies 0.°25 away from 4U 1630–472.

During the 2006 outburst, the Joint European X-Ray Monitor (JEM-X) of *INTEGRAL* observed the 4U 1630–472 field for a total of 14 ks. 4U 1630–472 was detected in the 3–7 keV mosaic image at flux level of 270 mCrab, while IGR J16320–4751 was not detected at all (an upper limit of a few mCrab; see left panel of Fig. 3). The latter source was instead clearly detected in the IBIS mosaic image of the same *INTEGRAL* observations at a flux level of 14 mCrab, while 4U 1630–472 was not detected at all (see Fig. 3, right panel). Looking at the All-Sky Monitor (ASM) and Burst Alert Telescope (BAT) light curves of IGR J16320–4751, we can see that, even though it is variable, the source is faint and does not show any particular increase of the flux during the three 4U 1630–472 outbursts.

We extracted the predicted PCA counts s^{-1} using the `ppms` tool and the detailed spectral analysis reported by Rodriguez et al. (2006). We considered the less favourable case in which the source is in a flaring state with a flux of 2×10^{-10} erg s^{-1} cm^{-2} (Rodriguez et al. 2006). Considering also the PCA response curve as a function of the off-axis position (Jahoda et al. 2006), we obtained a PCA count rate of 10 counts s^{-1}, a rate consistent with Tomsick et al. (2014). Thus, when 4U 1630–472 approaches 10 PCA counts s^{-1}, the contribution of IGR J16320–4751 is no longer negligible but can be considered almost constant. In fact, the flux variation of IGR J16320–4751 is quite limited and the source varies in flux but not in spectral shape (Rodriguez et al. 2006). The source spectra also present a Gaussian emission line, centred at 6.4 keV, and an iron edge (Rodriguez et al. 2006). Considering the continuum spectral shape of the IGR J16320–4751 flaring state as reported by Rodriguez et al. (2006), and the continuum spectral shape of 4U 1630–472 during the last PCA observations, we put a limit on spectral reliability at a conservative flux level of 4×10^{-10} erg s^{-1} cm^{-2} in the 2–10 keV energy range (which corresponds to ∼50 counts s^{-1}). Fig. 4 shows the comparison between the IGR J16320–4751 flaring spectrum as reported by Rodriguez et al. (2006) and the 50 counts s^{-1} 4U 1630–472 spectrum of the 2006 outburst.

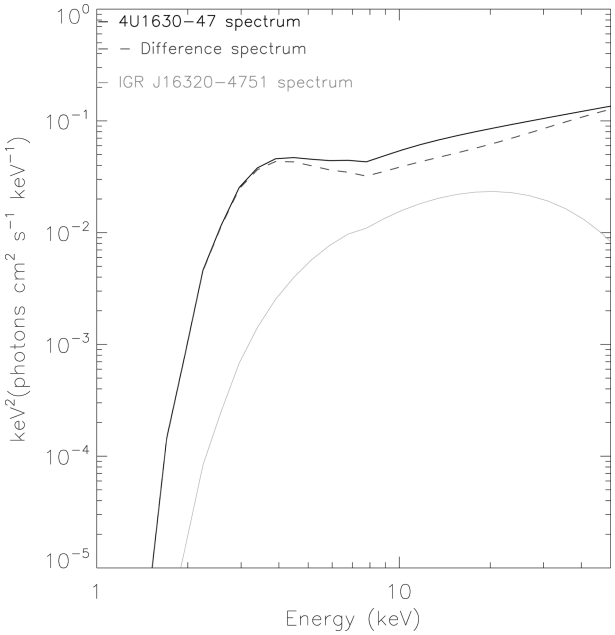

Figure 4. Comparison between the 2010 outburst unfolded spectral model of 4U 1630–472 at a flux level of 4×10^{-10} erg s^{-1} cm^{-2} (which corresponds to ∼50 counts s^{-1} in the 2–10 keV energy range) and the flaring state of IGR J16320–4751 (from Rodriguez et al. 2006). The plot also shows the difference between the two spectra (dark-grey dashed line).

During both 2006 and 2008 outbursts, 4U 1630–472 was not detected above 30 keV by *INTEGRAL*/IBIS and *Swift*/BAT (see, for example, the BAT light curve in Fig. 5 and the right panel of Fig. 3 for the 2006 IBIS outburst image). Thus, the *RXTE*/High-Energy X-ray Timing Experiment (HEXTE) spectra are irreparably contaminated by IGR J16320–4751, which instead, shows a bright emission above 30 keV, and therefore these have not been used in the subsequent analysis. During the 2010 outburst, *RXTE*/HEXTE was no longer in operation.

3 RESULTS

As Fig. 5 shows, the source light curve in the energy range 2–20 keV is very similar for the first two outbursts in 2006 and 2008, while the 2010 outburst presents a different time evolution showing two bright peaks in the light curves and reaching harder energy values. Fig. 6

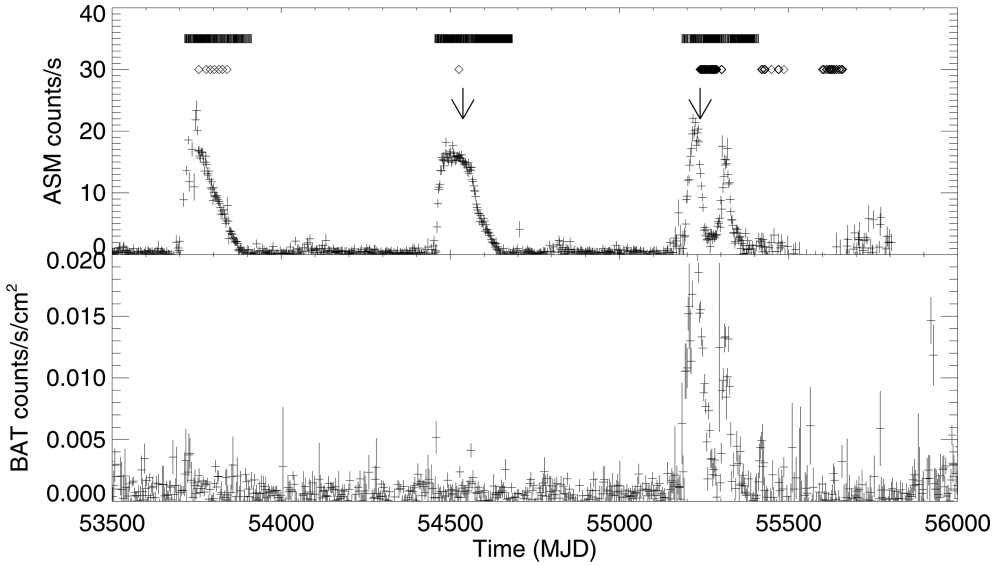

Figure 5. Top panel: 4U 1630–472 ASM light curve (bin size 2 d). The rectangles represent the PCA observation dates, the diamond points represent the *INTEGRAL* observations and the arrows correspond to the spectra in Figs 11–14 (see Section 3.4). Bottom panel: 15–50 keV *Swift*/BAT light curve (bin size 3 d). The 4U 1630–472 BAT 1σ detection sensitivity is 5.3 mCrab for a full-day observation, where 1 mCrab is 0.00022 count cm^{-2} s^{-1} (Krimm et al. 2013).

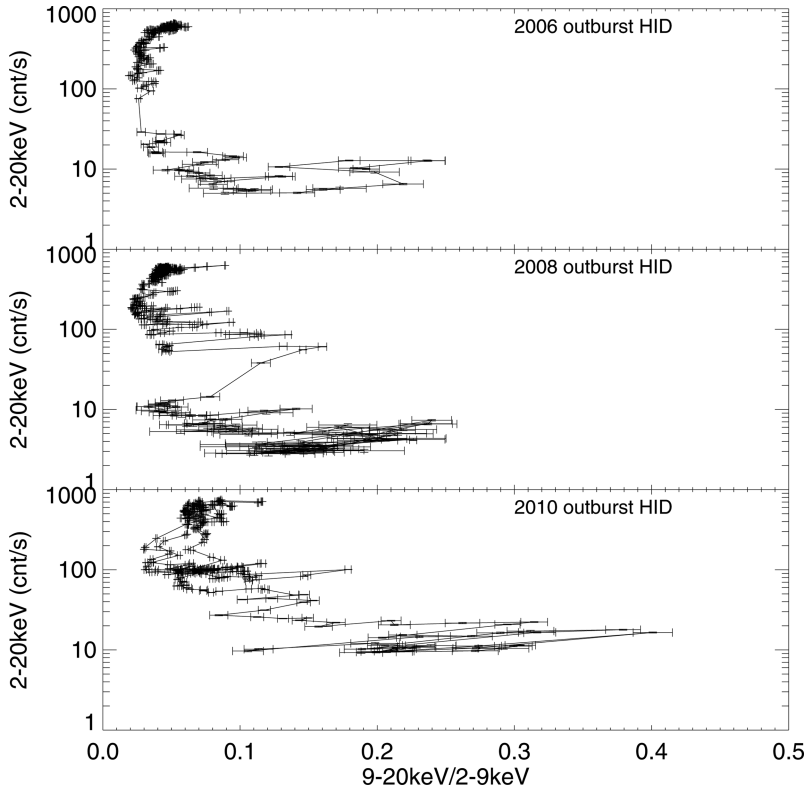

Figure 6. HIDs for the three outbursts: 2006 (top panel), 2008 (middle panel) and 2010 (bottom panel).

shows the *RXTE*/PCA hardness–intensity diagrams (2–20 keV versus 9–20 keV/2–9 keV, hereafter HIDs) of the three outbursts, while Fig. 7 shows the PCA light curve in two energy ranges (first two panels), the hardness ratio (HR) evolution as a function of time (third panel) and the evolution of the root mean square (rms) variability as a function of time (last panel). The dashed lines represent the time when the source goes below a PCA source flux of 50 counts s^{-1} – after this conservative limit, the contamination of IGR J16320–4751 can no longer be ignored. As Fig. 6 shows, the HIDs of the 2006 and 2008 outbursts are mostly identical, while the HID of the 2010 outburst evolves at higher energies. The 2010 outburst reaches 30 per cent greater values with respect to those reached during the 2006 and 2008 outbursts.

No hard X-ray emission is significantly detected for the 2006 and 2008 outbursts, as shown by the light curve taken from the BAT hard X-ray transient monitor on board the *Swift* satellite (Gehrels

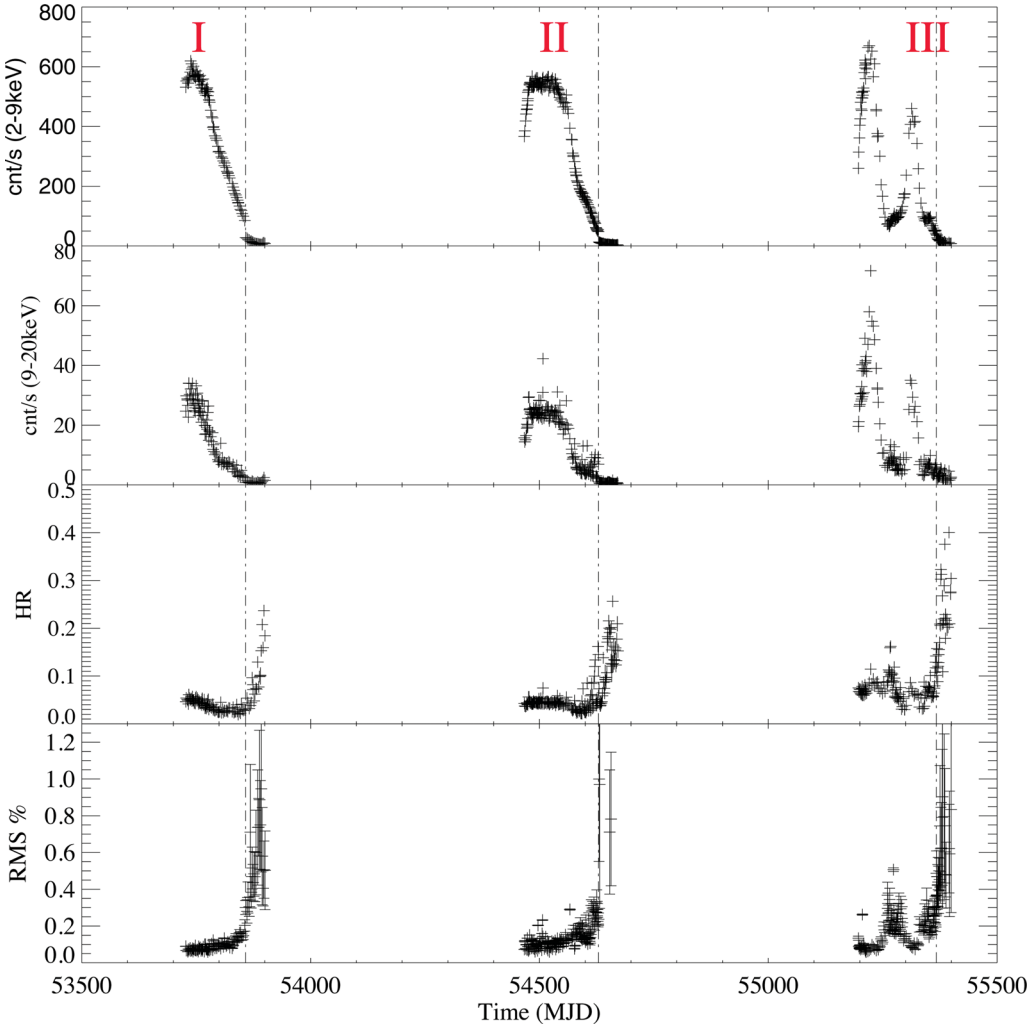

Figure 7. PCA light curves of the three outbursts, I, II and III: top panel, 2–9 keV; upper-middle panel, 9–20 keV; lower-middle panel, HR (9–20 keV/2–9 keV) versus time; bottom panel, fractional rms versus time. Each point corresponds to a PCA pointing. The dashed lines represent the time when the source reaches a count rate of 50 counts s^{-1} in the 2–10 keV energy range. After this limit, the contamination due to IGR J16320–4751 can no longer be ignored.

et al. 2004); see Fig. 5. In contrast, the BAT light curve of the 2010 outburst shows a flux about 14 times higher than that of the two previous outbursts.

The *INTEGRAL* data give similar results: no detections are present in the mosaic image of the IBIS data for both the 2006 and 2008 outbursts. The IBIS upper limit is 3 mCrab in 20–40 keV (for a total exposure time of 31 ks) for the 2006 outburst and 5 mCrab for the 2008 outburst (25 ks). The diamond points in Fig. 5 (top panel) show the *INTEGRAL* coverage of the three outbursts. In contrast, the JEM-X 2006 mosaic data show 4U 1630–472 as a moderately bright source (270 mCrab in the 3–7 keV energy range). The 2008 outburst is outside the JEM-X FOV. However, the ASM gives consistent results (the peak luminosity is at about 300 mCrab in 1–12 keV).

The IBIS mosaic image of the 2010 outburst shows 4U 1630–472 as a moderately bright source at flux levels of 20 mCrab (20–40 keV) and 83 mCrab (40–100 keV). The 2010 outburst is also outside the JEM-X FOV.

Considering the Fender, Belloni & Gallo (2004) classification – see also Belloni et al. (2005) for more details and Remillard & McClintock (2006) for an alternative classification of spectral states – the shapes of the power spectra, extracted from the PCA data taken during the three outbursts, are dominated by a power law and show that the source remains substantially in the high soft state (HSS) or intermediate soft state (see Figs 11–14 and Tables 2 and 3). However, because of the faintness of the source, the power spectra resolution does not allow us to determine the details of the power density spectrum (PDS).

3.1 Evolution of the 2006 outburst

The *RXTE* 2006 observation campaign started on 2005 December 23 (MJD 53727), about 15 d after the ASM flux enhancement (Tomsick 2005). Simultaneous observations with the Australia Telescope Compact Array (ATCA) performed on 2005 December 21, 25, 27 and 29 did not detect any radio counterpart of 4U 1630–472 on any of the four dates (Gallo et al. 2006). There is no evidence of enhanced flux in the BAT light curve all over the outburst (Fig. 5) and no detection in the IBIS data. Thus, the spectral analysis was focused on the PCA data collected during the 2006 outburst observation campaign.

After a brief enhancement, the 2–9 keV and 9–20 keV PCA fluxes decrease monotonically during the outburst, as shown in the first two panels of Fig. 7. The dashed line in Fig. 7 represents the limit

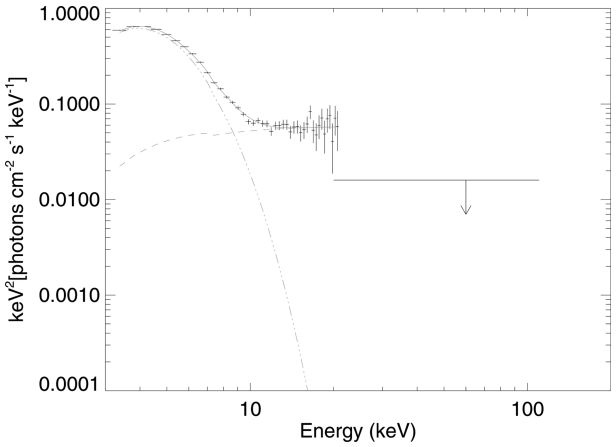

Figure 8. PCA unfolded spectrum of the 2006 outburst plus the IBIS upper limit (3 mCrab), obs. ID 91704-03-42-00. For model and fitting parameters, see Table 2. The dashed lines represent the single model components.

of 50 counts s^{-1}. As we have seen in Section 2.1, after this limit the contamination of the nearby source IGR J16320–4751 cannot be ignored. This corresponds to the last 23 pointings. The contamination due to IGR J16320–4751 is the cause of the huge hardening of the data in Fig. 7 (lower-middle panel). In any case, a slight hardening of the data (before the dashed lines) can be attributed to 4U 1630–472. Nevertheless, even in the last observations, when the power-law photon index decreases in value and the source spectra are harder, the *F*-test strongly indicates that a disc blackbody component is still needed in the spectral models to provide a good fit (*F*-test probabilities $<10^{-5}$).

The evolution of the most significant fit parameters along the 2006 outburst is plotted in Fig. 9(a). The disc blackbody emission dominates the spectrum for two and a half months ($T_{\rm in} \sim 1.3$ keV). Then, the inner temperature of the disc starts to decrease together with the flux, reaching inner temperatures of about ∼0.8 keV. Thereafter, the contamination of the nearby source can no longer be neglected. The power-law photon index, instead, reaches extremely soft values even considering the huge errors. This happens when the high-energy flux (20–30 keV) is below 4×10^{-11} erg cm^{-2} s^{-1}. In these spectra, the power-law component – even though it is required in order to obtain a good fit – is so small that a systematic error in the determination of the photon index cannot be excluded.

During the second part of the outburst, the power-law photon index hardens and remains mostly constant at values of ∼1.8. Moreover, there is no evidence in the data of a power-law cut-off until 30 keV. These spectral parameters are compatible with a soft state as indicated by the PDS.

However, because the PCA spectra reach only 30 keV and there are no detections of the source in IBIS and BAT data (both instruments share a similar upper limit of a few mCrab), we can impose, with good confidence, that there should be a cut-off at energies around 30 keV. To demonstrate this fact, Fig. 8 shows, as an example, the PCA spectrum of the observation 91704-03-42-00 plus the IBIS upper limit. This figure clearly shows that the lack of a cut-off should imply a detection, at least by one of the two instruments, IBIS and BAT.

We also applied to the high-energy part of the data, instead of the power law, two simple physical models describing Comptonization of soft photons in a hot plasma, Models 2 and 3 (see Section 2). Because of the lack of a cut-off in the data, the electron plasma temperature parameter could not be defined by the fitting procedure.

Then, because the energy cut-off is roughly $E_{\rm c} \sim 2$–$3\ kT_{\rm e}$ (see Petrucci et al 2001; Miyakawa et al. 2008, and references therein), we fixed the plasma temperature at 15 keV. With this condition, the spectral parameters of Model 2 are consistent within the errors with those of Model 1. The Model 3 plasma optical depth increases, together with the hardening of the source, with values within the range 0.4–4.3 (see Fig. 9), whereas the softest spectra are mostly dominated by the disc blackbody and the plasma optical depth is quite low (∼1). It is worth noticing that the COMPTT model, used to model the high-energy part of the spectra in Model 3, is not valid for simultaneously low temperatures and low optical depth. In fact, for $kT_{\rm e} = 15$ keV and low values of τ ($\leq$1), the corresponding values of the β parameter (Titarchuk 1994) are outside the zone of applicability of the model (Hua & Titarchuk 1995, fig. 7).

3.2 Evolution of the 2008 outburst

The *RXTE* observation campaign started on 2008 January 01 (MJD 54466), about 6 d after the first ASM detection (Kalemci et al. 2008). There is no evidence of either flux enhancement in the BAT light curve or detection in the IBIS data. Thus, no hard X-ray emission is detected above 30 keV as in the case of the 2006 outburst. Also for this outburst, the spectral analysis was focused on all the data collected from the PCA during the 2008 outburst.

The evolution of the two most significant fit parameters during the whole 2008 outburst is plotted in Fig. 9(b). The behaviour of this outburst substantially retraces the 2006 outburst. After a rapid enhancement, the disc blackbody emission dominates the spectrum for the first three months ($T_{\rm in} \sim 1.3$ keV). Then, the inner temperature of the disc blackbody decreases monotonically during all the outburst together with the source flux. As for the previous outburst, during the softest part of the spectral evolution, the power-law photon index reaches extremely soft values. This happens when the disc blackbody emission dominates the spectrum and the high-energy flux (20–30 keV) is below 3×10^{-11} erg cm^{-2} s^{-1}. There is no evidence in the data of a power-law cut-off until 30 keV, even though, in analogy with the 2006 outburst, the lack of IBIS and BAT detection indicates a cut-off just above 30 keV (see Fig. 11).

During the last PCA pointings, there is evidence of an increase in both the rms and the HR values (Fig. 7). However, the *F*-test strongly indicates that in these observations a disc blackbody component is needed in the spectral models to obtain a good fit (*F*-test probability $<10^{-3}$). The spectral parameters reported in Fig. 9(b) are compatible with a soft state of the source, as indicated by the PDS. In the last 45 pointings, the contamination of the nearby source cannot be ignored (see dashed line in Fig. 9b).

We also applied to the data the same models used for the 2006 outburst observations (Models 2 and 3 as defined in Section 2), fixing the plasma temperature at 15 keV. As for the previous outburst, the Model 2 spectral parameters are consistent within the errors with those of Model 1, whereas the Model 3 plasma optical depth increases together with the hardening of the source. The softest spectra are mostly dominated by the disc blackbody, so it is impossible to fit the high-energy data even with a simple Comptonization model. As the bottom panel of Fig. 9 shows, during the 2008 outburst the optical depth reaches values comparable with the 2006 outburst ($0.4 < \tau_{\rm p} < 4.5$). Also, in this case, values of τ lower than 1 are outside the zone of applicability of the model (Hua & Titarchuk 1995).

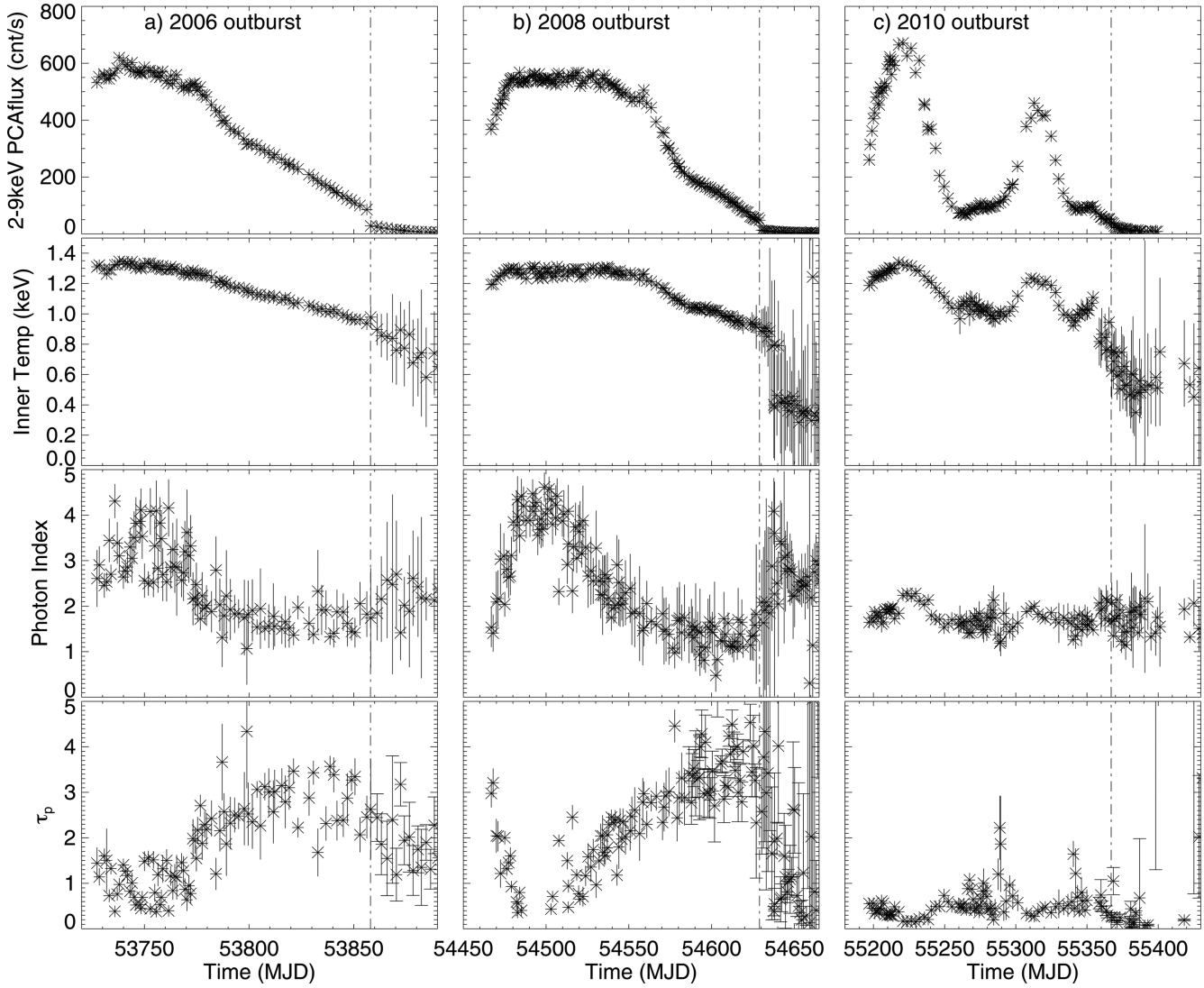

Figure 9. The flux and fit parameter evolution of Model 1 for the 2006, 2008 and 2010 outbursts: WABS × (DISKBB+POW) ($\tilde{\chi}^2_{\rm red} = 1.0$, $0.5 < \chi^2_{\rm red} < 1.9$). The bottom panels represent the evolution of the plasma optical depth, $\tau_{\rm p}$, of Model 3: WABS × (DISKBB+COMPTT). The dashed lines represent the flux limit after which the contamination of the nearby source, IGR J16320–4751, cannot be neglected. Each point of the figures represents the value of a spectral parameter of a single PCA observation.

3.3 Evolution of the 2010 outburst

On 2009 December 29 (MJD 55194), the gas slit camera (GSC) of the Monitor of All-sky X-ray Image (MAXI) detected an increase in X-ray intensity from 4U 1630–472 (Tomida et al. 2009). Five days later, a radio observation campaign was carried out with the ATCA telescope, consisting of two pointings (1440 s per observation). Once again, also during the 2010 outburst, the radio emission of the source was below the detection limit of the instrument, 93 and 126 μJy at 5.5 and 9 GHz, respectively (Calvelo et al. 2010). The *RXTE* observation campaign started on 2010 January 01. This outburst was observed by *INTEGRAL* for a total IBIS exposure time of about 700 ks simultaneous with *RXTE*.

The PCA spectral parameter evolution reported in Fig. 9(c) and the enhancement of the emission above 15 keV (see the *Swift*/BAT light curve in Fig. 5) give an indication of two subsequent softenings of the source with an increase of both the inner temperature and the power-law photon index (Fig. 9c). Nevertheless, during the source hardenings, subsequent to the two soft peaks, the contribution of the disc emission remains prominent, according to Tomsick et al. (2014), and the average photon index value remains at ∼1.7.

Just to the end of the 2010 outburst and in spite of the IGR J16320–4751 contamination, the PCA data show a slight hardening of the source (see, for example, the HR and rms in Fig. 5). No power-law cut-off is detected in the IBIS data up to 150–200 keV. Therefore, the greatest difference between this outburst and the previous two is the bright emission above 30 keV (Fig. 5).

We also applied to the high-energy part of the spectra, instead of a power law, the same Comptonization models used for the two previous outbursts. In this case, we fixed the plasma temperature at 100 keV because of the BAT continuous detection of the source during the 2010 outburst and because of the PCA–IBIS joint spectra fit results that do not allow us to constrain any cut-off until 150–200 keV. However, we cannot exclude that, when IBIS was not observing the source, a cut-off could be present at energies lower than 200 keV but greater than 30 keV. The Model 2 spectral parameters are consistent within the errors with those of Model 1,

Table 1. The 2010 outburst spectral evolution of the 13 PCA–IBIS joined spectra of 4U 1630–472. The best-fitting model is CONST*WABS*(DISKBB+PEXRAV). Rev denotes the IBIS revolution number. $N_{\rm H}$ is the equivalent hydrogen column, free to vary in the range 4–12 $\times$ 10^{22} cm^{-2}, previously reported in the literature (e.g. Trudolyubov et al. 2001; Tomsick et al. 2005). $T_{\rm in}$ is the temperature of the inner disc. $N_{\rm disc} = [(R_{\rm in}/{\rm km})/(D/{\rm kpc})]^2$ is the normalization parameter of the Sakura–Sunyaev disc blackbody. Γ is the power-law photon index. $Rel_{\rm refl}$ is the reflection scaling factor (the cosine of inclination angle is left fixed at its default value, 0.45). $F_{2-10\,{\rm keV}}$ is the unabsorbed flux between 2 and 10 keV. $F_{10-100\,{\rm keV}}$ is the unabsorbed flux between 10 and 100 keV. $\chi^2_{\rm r}$ is the reduced χ^2. The last line shows the spectral parameter of the averaged IBIS spectrum of the last part of the outburst fitted with a simple power law (see Section 3.3).

Rev	Obs. date MJD	IBIS exp. (ks)	$N_{\rm H}$ (10^{22} atm cm^{-2})	$T_{\rm in}$ (keV)	$N_{\rm disc}$	Γ	$Rel_{\rm refl}$	$F_{2-10\,{\rm keV}}$ (erg cm^{-2} s^{-1})	$F_{10-100\,{\rm keV}}$ (erg cm^{-2} s^{-1})	χ^2_r(d.o.f.)
895	55239	14	$7.3^{+0.3}_{-0.3}$	$1.22^{+0.02}_{-0.02}$	190^{+24}_{-21}	$2.2^{+0.1}_{-0.1}$	<0.2	5.1e-09	1.4e-09	0.8 (77)
896	55241	18	$8.1^{+0.3}_{-0.3}$	$1.20^{+0.01}_{-0.01}$	177^{+20}_{-18}	$2.1^{+0.1}_{-0.1}$	$0.5^{+0.3}_{-0.3}$	5.1e-09	1.4e-09	1.1 (66)
897	55244	15	$7.8^{+0.3}_{-0.3}$	$1.16^{0.01}_{-0.01}$	170^{21}_{-19}	$2.0^{+0.1}_{-0.1}$	$0.5^{+0.4}_{-0.3}$	4.1e-09	1.1e-09	1.1 (70)
897,898	55247	16	$6.4^{+0.4}_{-0.4}$	$1.12^{+0.02}_{-0.02}$	126^{+22}_{-19}	$2.0^{+0.1}_{-0.1}$	$0.4^{+0.4}_{-0.3}$	2.7e-09	8.8e-10	1.4 (73)
898	55248	14	$6.3^{+0.3}_{-0.3}$	$1.10^{+0.02}_{-0.02}$	120^{+24}_{-21}	$1.7^{+0.2}_{-0.1}$	<0.3	2.2e-09	7.3e-10	1.2 (73)
899,900	55252	44	$6.2^{+0.5}_{-0.5}$	$1.04^{+0.02}_{-0.02}$	100^{+23}_{-18}	$2.0^{+0.1}_{-0.1}$	$0.6^{+0.5}_{-0.3}$	1.5e-09	5.2e-10	1.2 (74)
901	55257	26	$5.3^{+0.5}_{-0.5}$	$1.03^{+0.02}_{-0.02}$	84^{+25}_{-19}	$1.8^{+0.2}_{-0.1}$	<0.4	1.1e-09	4.0e-10	1.1 (70)
901,902	55259	32	5^{+1}_{-1}	$0.98^{+0.03}_{-0.04}$	86^{+36}_{-25}	$2.2^{+0.2}_{-0.3}$	$1.5^{+1.2}_{-0.9}$	1.0e-09	3.7e-10	1.3 (72)
902,904,905	55265	16	<4	$1.1^{+0.1}_{-0.1}$	32^{+17}_{-11}	$2.0^{+0.1}_{-0.1}$	$0.6^{+0.5}_{-0.4}$	6.7e-10	4.3e-10	0.8 (72)
906,907	55272	72	$5.4^{+0.6}_{-0.6}$	$1.03^{+0.03}_{-0.03}$	105^{+31}_{-23}	$2.1^{+0.1}_{-0.1}$	$0.8^{+0.5}_{-0.4}$	1.6e-09	4.9e-10	1.0 (70)
907,908	55276	79	$5.8^{+0.6}_{-0.5}$	$1.01^{+0.02}_{-0.02}$	111^{+28}_{-22}	$1.9^{+0.2}_{-0.1}$	$0.8^{+0.6}_{-0.4}$	1.3e-09	3.8e-10	1.4 (70)
909,910,911	55284	128	7^{+1}_{-1}	$0.9^{+0.03}_{-0.03}$	121^{+47}_{-36}	$2.0^{+0.2}_{-0.1}$	<0.6	1.3e-09	2.6e-10	0.8 (72)
916	55302	95	$8.5^{+0.4}_{-0.4}$	$1.1^{+0.01}_{-0.01}$	266^{+45}_{-38}	$1.9^{+0.1}_{-0.1}$	<0.4	4.7e-09	6.1e-10	0.8 (70)
956–959–965	55420–55449	78	–	–	–	$2.1^{+0.3}_{-0.3}$	–	–	2.3e-10	0.6 (26)

whereas the bottom panel of Fig. 9 shows the Model 3 plasma optical depth evolution. The optical depth slightly increases when the spectra hardens but its variation is less important with respect to the values reached during the two previous outbursts.

Even though we do not consider the high-energy cut-off, the accuracy of the joint PCA–IBIS spectra is not sufficient to discriminate between thermal, non-thermal or hybrid electron distribution using more refined Comptonization models such as COMPPS.

Because of the broad-band spectra and the higher emission above 30 keV, we also attempt to fit the joint PCA–IBIS data of the 2010 outburst, taking into account the reflection component. The model used for the fitting procedure was introduced in Section 2 as Model 4. The joint spectra (see the top panel of Fig. 5) are mostly concentrated during the declining phase of the first soft peak of the 2010 outburst. Table 1 reports the evolution of all the PCA–IBIS spectral parameters. The PCA–IBIS spectral resolution is not sufficient to constrain the reflection component well, which has large errors or can even be defined only with an upper limit. For the spectra where the reflection component is constrained by the data (even though with huge errors) the *F*-test probability indicates that the fit is improved (*F*-test probabilities $<4 \times 10^{-3}$). An alternative view reported by Laurent & Titarchuk (2007) and based on bulk motion photon propagation, demonstrates, using Monte Carlo simulations, that for $\Gamma > 2$ there is no bump in the reflection spectrum due to downscattering accumulation of photons from the high-energy tail of the incident spectrum.

Our results obtained from the 13 joint PCA–IBIS spectra are consistent with $\Gamma \leq 2$ with the exception of the first observation for which the reflection component is not constrained (see Table 1). Even though far from conclusive, our results are supported by King et al. (2014), who report the clear presence of a reflection component in the intermediate state of the 2013 source outburst during a short *NuSTAR* observation.

The *INTEGRAL* observations continued after the end of the *RXTE* pointings. The last line of Table 1 shows that the source persisted in having a spectrum extending at high energies that can be fitted with good confidence with a power law ($\Gamma \sim 2$) without cut-off until 150–200 keV. Unfortunately, there are no data below 20 keV because the source was outside the JEM-X FOV.

3.4 Comparison of the three outbursts

The top panel of Fig. 1 shows the long-term light curve between 2 and 4 keV of all the outbursts detected by the *RXTE*/PCA from 1996 until 2011, while the bottom panel shows the HR, defined as the ratio between the 4–9 keV and 2–4 keV energy ranges, versus time. The bottom panel of Fig. 1 indicates that the 2006 and 2008 outbursts reached the softest HR values with respect to the 2010 outburst, and also with respect to all the previous outbursts observed by *RXTE*, including the outbursts with similar luminosity (e.g. the 2001 outburst, MJD 52000 in Fig. 1)[1] that are reported in that literature as standard outbursts (Dieters et al. 2000; Trudolyubov et al. 2001).

In order to highlight the differences between the two 2006 and 2008 outbursts and the 2010 outburst, we present, as an example, the energy and the power spectrum of two PCA observations: the first was performed during the 2008 outburst and the second during the 2010 outburst. Fig. 11 shows the energy spectrum of the 2008 PCA observation 93425-01-11-07 and the 25-ks IBIS upper limit; Fig. 12 shows the power spectrum of the same PCA observation. Fig. 13 shows, instead, the energy spectrum of the 2010 PCA observation 95360-09-24-00 with the simultaneous IBIS spectrum, while Fig. 14 shows the relative PCA power spectrum.

The two PCA observation dates correspond to the black arrows in Fig. 5 and exhibit the same source state: a similar spectral shape between 2 and 20 keV, a similar rms value, a similar power spectrum and a similar 2–20 keV flux emission, as Tables 2 and 3 show.

[1] The ASM HR versus time plot gives the same results.

Table 2. Fit parameters of the two energy spectra plotted in Figs 11 and 13. The best-fitting model is CONST*WABS*(DISKBB+POW). PCA obs. ID is the PCA observation number. T_{in} is the temperature of the inner disc. $N_{disc} = [(R_{in}/km)/(D/kpc)]^2$ is the normalization parameter of the Sakura–Sunyaev disc blackbody. Γ is the power-law photon index. N_{pow} is the normalization parameter of the power-law model. The hydrogen column density is left free to vary between 4 and 12 $\times$ 10^{22} atm cm^{-2}, as previously reported by Tomsick et al. (1998).

PCA obs. ID	T_{in} (keV)	N_{disc}	Γ	N_{pow} (ph keV^{-1} cm^{-2} s^{-1})	$Flux_{2-10\,keV}$ (erg cm^{-2} s^{-1})	$Flux_{10-100\,keV}$ (erg cm^{-2} s^{-1})	χ^2_{red}(d.o.f.)
93425-01-11-07	1.31±0.01	340±13	2.3±0.2	$0.3^{+0.2}_{-0.1}$	1.3×10^{-8}	–	1.1(52)
95360-09-24-00	1.21±0.02	243^{+20}_{-18}	2.2±0.1	1.0±0.2	0.8×10^{-8}	1.9×10^{-9}	0.8(66)

Table 3. Fit parameters of the two power spectra plotted in Figs 12 and 14. The best-fitting model is (power law+Lorentzian). PCA obs. ID is the PCA observation number. Γ is the power-law photon index. E_L is the Lorentzian line energy. σ is the Lorentzian FWHM linewidth.

PCA obs. ID	Γ	E_L (keV)	σ (keV)	rms	χ^2_{red}(d.o.f.)
93425-01-11-07	1.7±0.2	$1.2^{+0.4}_{-1.2}$	1.7^{+4}_{-1}	0.091	0.8(13)
95360-09-24-00	$2.1^{+0.5}_{-0.3}$	$1.4^{+0.6}_{-1}$	2.6^{+2}_{-1}	0.067	0.5(12)

Above 30 keV, instead, there is a pronounced difference. In fact, for the 2010 outburst, the data above 30 keV can be fitted with a power law and no cut-off is required in the model to fit the data up to 250 keV. Also, for the 2008 outburst, a power-law component is needed in the model to obtain a good fit until 30 keV. However, as we have demonstrated in Sections 3.2 and 3.2, the non-detection of the source at a higher energy range implies that there should be a cut-off just above 30 keV. Moreover, the huge difference in value, between the power-law normalization parameter of the two spectra, indicates that for the 2008 outburst the contribution of the power law in the spectrum is lower than in the case of the 2010 outburst, while the apparent inner radius extracted from the normalization constant of DISKBB is 26 and 30 km, respectively; see Kubota et al. (1998) for the correction factor between the apparent inner disc radius and the realistic radius.

All three outbursts seem not to follow the two empirical relations, reported by Yu & Yan (2009), Yu et al. (2007) and Wu et al. (2010), between the hard X-ray luminosity peak of the HS to the HSS transition and the HSS luminosity peak, and between the hard luminosity peak and the outburst waiting time, respectively. In fact, following the relation reported by Wu et al. (2010), a constant waiting time, which is a peculiarity of 4U 1630–472, should imply a constant hard X-ray luminosity peak of the subsequent outburst. This relation is not verified between the 2008 and 2010 outbursts, or between the 2002–2004 and 2006 outbursts (Fig. 1). Concerning the relation occurring between the X-ray HS to HSS transition luminosity peak versus the subsequent HSS luminosity peak, Fig. 10 shows that the 2006 and 2008 outbursts are totally outside the correlation reported by Wu et al. (2010) (grey filled zone in Fig. 10). In fact, the HS–HSS transition should have occurred before the start of the PCA observation campaign. On the contrary, the 2010 outburst is almost in agreement, emphasizing that the lack of hard X-ray emission in the case of the 2006 and 2008 outbursts is unusual.[2]

[2] We consider as the hard to soft transition flux peak of the 2010 outburst the BAT 15–50 keV luminosity taken on 2009-12-29, which corresponds to the first detection of the outburst (Tomida et al. 2009). In fact, just two days later on 2009-12-31, the source exhibits a spectral behaviour typical of HSS (Tomsick, Shaposhnikov & Swank 2009).

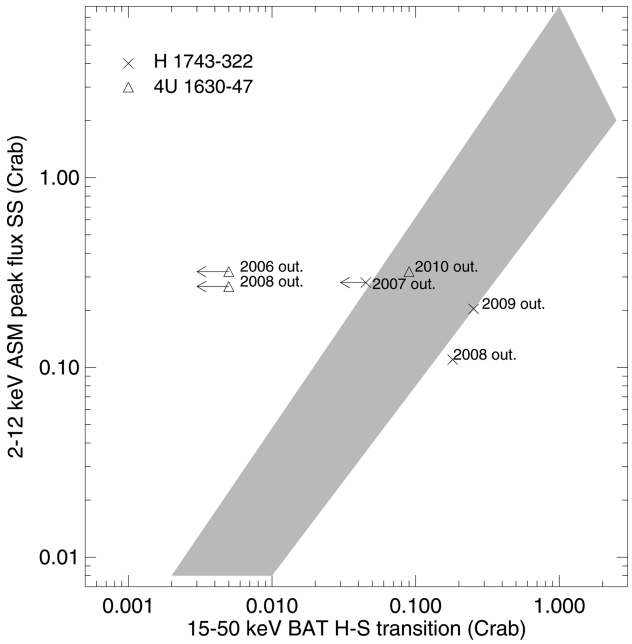

Figure 10. BAT flux during the hard to soft transition versus the corresponding ASM flux of 4U 1630–472 and H 1743–322 as defined in Yu & Yan (2009). The grey zone represents the region populated by other BHXRBs reported by Yu & Yan (2009).

In order to understand the uniqueness of the recurrence of the 4U 1630–472 outbursts and to correlate this with the lack of high-energy emission, we investigated the ASM and BAT light curves of some of the brightest and active transient black hole X-ray binaries (BHXRBs) during the seven years (2005–2011) in which both instruments were operational. Many studies of the outburst evolution of these sources have been reported in the literature (e.g. Yu & Yan 2009; Capitanio et al. 2010; Dunn et al. 2010, and references therein); the various outbursts observed do not have any detectable recurrence period and, in addition, show a complex behaviour in both soft and hard energy ranges and very different luminosities. The only exception is H 1743–322; this BHC has shown only for some years outbursts equally spaced in time, as reported by Capitanio et al. (2010). In analogy with 4U 1630–472, the outburst of H 1743–322 that occurred in 2007 has a 2–12 keV behaviour mostly identical to some of the subsequent periodical outbursts but showing a fainter hard X-ray emission; the H 1743–322 ASM 2007 peak flux (1–12 keV) is ∼250 mCrab and the BAT 2007 peak flux (15–50 keV) is ∼60 mCrab. The subsequent H 1743–322 outburst (2008–2010) presents a similar 1–12 keV flux but with a 15–50 keV flux of ∼200 mCrab. As Fig. 10 shows, the difference in the ratio between the BAT HS–HSS transition luminosity and the ASM peak flux of H 1743–322 is not enough to bring the outburst totally out

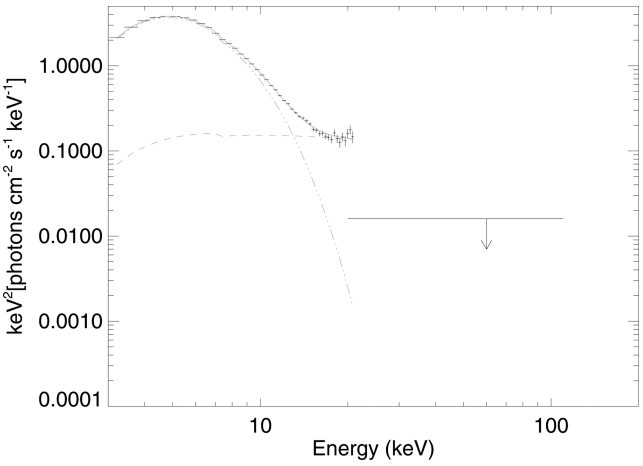

Figure 11. PCA unfolded spectrum of the 2008 outburst plus the IBIS upper limit (5 mCrab), Obs. ID 93425-01-11-07. For model and fitting parameters, see Table 2. The dashed lines represent the single model components.

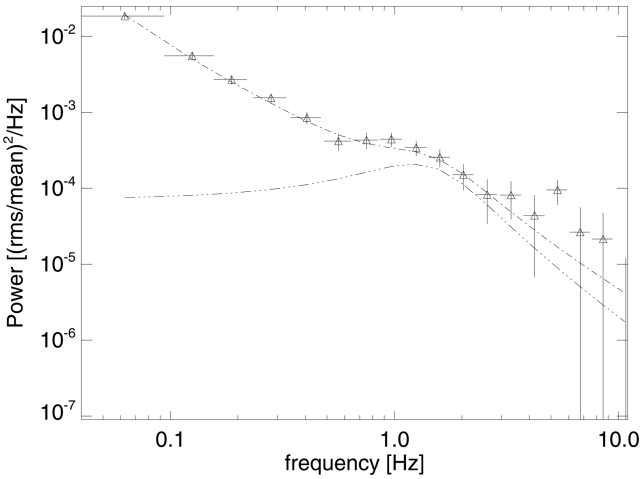

Figure 12. PCA power spectrum of the 2008 outburst. The rms value is 0.091 (see Section 2 for details), Obs. ID 93425-01-11-07. For model and fitting parameters, see Table 3. The dashed lines represent the single model components.

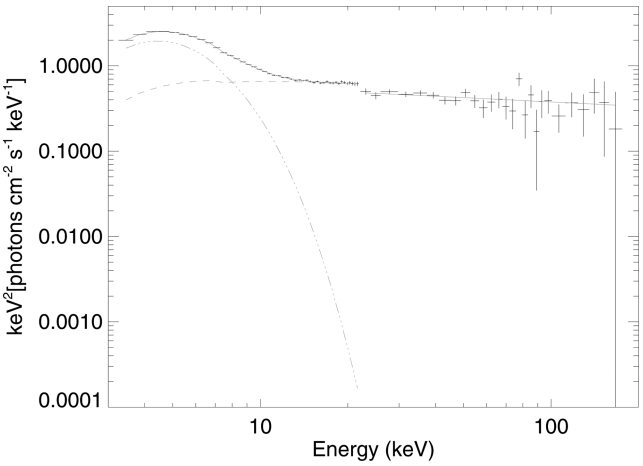

Figure 13. PCA–IBIS unfolded joint spectrum of the 2010 outburst, Obs. ID 95360-09-24-00. For model and fitting parameters, see Table 2. The dashed lines represent the single model components.

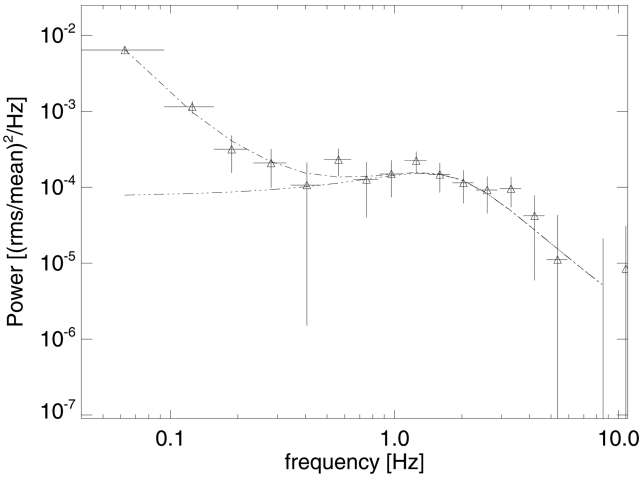

Figure 14. PCA power spectrum of the 2010 outburst. The rms value is 0.067 (see Section 2 for details), Obs. ID 95360-09-24-00. For model and fitting parameters, see Table 3. The dashed lines represent the single model components.

of the correlation reported by Yu & Yan (2009) as in the case of the 2006 and 2008 outbursts of 4U 1630–472. However, as reported by Corbel & Tzioumis (2008), the HS–HSS transition occurred before the peak of the hard X-ray emission and thus it is only an upper limit. For the 2007 and 2008–2010 outbursts of H 1743–322, the relation between the hard X-ray luminosity peak and the outburst waiting time is also not respected. In contrast, during the subsequent outbursts, a similar waiting time corresponds to a similar peak luminosity in the 15–50 keV energy range.

4 DISCUSSION

4.1 2006 and 2008 outbursts

The 2006 and 2008 outbursts are very similar to each other with respect to the flux emission, the outburst duration and the spectral evolution. Although the PCA observation campaign began immediately after the *RXTE*/ASM flux enhancement, there is no evidence in the data of both outbursts of the initial transition from the hard state to the soft state, as clearly indicated by the HID, the HR and the rms behaviour (see Figs 6 and 7). Thus, the initial transition should have occurred shortly after the beginning of each outburst or has not occurred at all. In support of this hypothesis, since the first observation of the ATCA campaign, performed at the beginning of the 2006 outburst on 2005 December 21 (Gallo et al. 2006), did not detect any radio emission. The quenching of the radio emission is typical of HSS; see, for example, Fender et al. (1999), Fender (2006), Russell et al. (2011) and Gallo et al. (2012) for a review of radio properties of XRBs. Besides, it is well known that 4U 1630–472 emits in the radio band, as mentioned in Section 1, during the 2002–2004 and 2013 outbursts and also during the 1998 outburst when 4U 1630–472 shows X-ray luminosity comparable with the 2006 and 2008 outbursts (see Fig. 1).

For the 2006 outburst, the radio non-detection fixes with good confidence that 4U 1630–472 probably reached the soft state very sharply. In fact, the first radio observation was performed only 7 d after the first ASM-confirmed detection (Tomsick 2005) and 11 d before the first PCA observation (2006 January 01).

Another unusual behaviour connects these two outbursts: the lack of any detection above 30 keV all the total duration of the outburst.

The data show a hardening of the 3–30 keV spectra during the final phase of the two outbursts, which corresponds to an increase of the rms in agreement with that expected for a BHXRB coming back to the low–hard state (LHS; Muñoz-Darias, Motta & Belloni 2011), even though the final LHS, if it occurs, is not detected in the data. In fact, the disc blackbody component is always required in the model to fit the data, and the power-law component, even though very faint, seems to be typical of a soft state, at least until 30 keV. Above 30 keV the non-detection implies the presence of an energy cut-off in the power law that is, instead, not typical of a soft state. However, the source flux drops rapidly, and thus the final hard state transition is probably under the detection threshold of IBIS and BAT, and the PCA data are contaminated by the nearby source IGR J16320–4751.

The lack of a bright hard state has also been observed previously in 4U 1630–472 (see Tomsick et al. 2005, and references therein). This is unexpected behaviour; although the LHS–HSS transition can occur at different luminosity levels (e.g. Maccarone 2003, and references therein), the initial LHS–HSS transition should occur at a luminosity about a factor of a few larger than the final HSS–HS transition (Zdziarski & Gierlinski 2004). Thus, if the initial transition is below the BAT detection sensitivity (10.6 mCrab for 1 d of observations at 2σ), the final hard state should be really subluminous ($<$ 0.5–0.05 mCrab) and near to the quiescent luminosity. An explanation could simply be that the initial transition was not so subluminous, but instead it was so sharp that the hard X-ray monitors (IBIS and BAT) did not have enough exposure time to detect it, while the PCA observation campaign started too late to observe the LHS. This is a possibility that does not involve any breaking of the hysteresis-like cycle of the HID (Zdziarski & Gierlinski 2004; Homan & Belloni 2005). It remains to be explained why the high-energy emission that is thought to be due to the inverse Compton was so faint during these two outbursts.

As demonstrated in the discussion above, the PCA energy and power spectra indicate that the source should be in a soft or intermediate soft state during the observation campaign.

Hence, according to Zdziarski & Gierlinski (2004), the accretion disc should be extended near the last stable orbit and the electron corona located in active regions on the disc surface. In this state, we expect non-thermal or hybrid distributions of the corona electrons. This implies, at first approximation, the presence in the spectral model of a power law without cut-off. Therefore, the presence of this power-law component in the 3–30 keV spectra and the lack of any detection above 30 keV, implies, instead, a cut-off at energies no higher than 30 keV. This could imply that the corona should have been, for some unknown reasons, quickly thermalized or it has not heated up at all at the beginning of the outburst, leading to a very low electron temperature, roughly $kT_{\rm e} \leq 15$ keV (Petrucci et al 2001; Miyakawa et al. 2008).

However, the evolution of the plasma optical depth, $\tau_{\rm p}$, is strongly related to the fixed value of the plasma temperature $kT_{\rm e}$. In fact, the only information that can be extrapolated from the data is that $kT_{\rm e}$ should be less than about 10–15 keV, but its variation during the two outbursts is totally unknown.

4.2 2010 outburst

The scenario is different in the case of the 2010 outburst. As in the two previous outbursts, the lack of any radio detection (Calvelo et al. 2010) probably implies a very sharp transition to the HSS, just 5 d before the first MAXI telescope detection reported by Tomida et al. (2009). However, the source brightens above 30 keV not during the hard state, if it occurs, but rather during the soft part of the outburst. In fact, as can be easily seen in Fig. 5, both the soft and hard light curves (top and bottom panels, respectively) reach the peak of emission at the same time. Normally, the hard peak of the X-ray light curve (i.e. 15–50 keV) precedes the soft peak (2–12 keV).

Either way, we can argue that the inverse Compton emission, during the 2010 outburst, is more efficient than in the previous two cases. The PCA–IBIS joint spectra do not present any cut-off of the power law until 150–200 keV. This means that just from the beginning of the outburst, the electron plasma temperature is very high or the electrons have a non-thermal distribution (Malzac & Belmont 2009), in agreement with the standard behaviour of BHXRBs in the soft state (e.g. Zdziarski & Gierlinski 2004). However, the spectral resolution does not permit us to distinguish the two cases. Nevertheless, as reported by Tomsick et al. (2014), the 2010 outburst shows another peculiarity: an anomalous delay of the final transition to the LHS. However, the last IBIS data, simultaneous with the *Suzaku* observations reported by Tomsick et al. (2014), do not show the typical LHS high-energy spectrum above 20 keV. In fact, the power law remains quite soft ($\Gamma \sim 2$) and there is no cut-off up to 150–200 keV. It is also true that the faintness of the data force too large integration time and the harder data, observed simultaneously with the transition, could have been averaged out with the other observations. Data obtained with smaller integration times around the date of the HSS to LHS transition are not statistically significant.

4.3 Periodical outbursts

The recurrence of an outburst every 600–700 d could be caused by a perturbation of periodical nature, which could force the system to undergo an outburst.

We argue that there is a connection between this periodicity of the outbursts and the peculiarity of their behaviour. In fact, the outbursts are thought to be caused by a variation of the mass accretion rate from the companion star via Roche lobe overflow. This variation causes an increase of the disc temperature inducing the ionization instability of the disc. In the case of 4U 1630–472, there should be an extra perturbation of the system that periodically triggers this variation. This perturbation forces an increase of the disc temperature independent of the mass accretion rate of the companion star and from the state of the accretion disc and the relativistic electrons inflow. This scenario could explain also the anomalies of the LHS–HSS and HSS–LHS transitions of 4U 1630–472 and the lack of a bright hard state. In fact, as demonstrated by Homan et al. (2001), while the variation in the mass accretion rate should cause the outbursts, the corona inflow seems to be involved in the state transitions of BHXRBs. Thus, we could argue that the forced outbursts do not respect all the steps that are involved in the hysteresis-like behaviour of the standard outbursts of BHXRBs.

Following this scenario, the 2002–2004 bright outburst (Fig. 1) could be considered a standard outburst of 4U 1630–472 due to the variation of the mass accretion rate of the companion star. This outburst covers a time period for which the source should have undergone an outburst two times. Surprisingly, the two bright flux peaks of this outburst lie exactly at the epochs in which we should expect two periodical outbursts (see Fig. 1). This fact fixes with good confidence that the unknown periodic perturbation was still active during the outburst and not related to the outburst origin.

In the last 20 yr, a wide variety of hypotheses have been put forward to explain the nature of the periodical perturbation. Here, we critically review all the hypotheses, trying to find the most plausible.

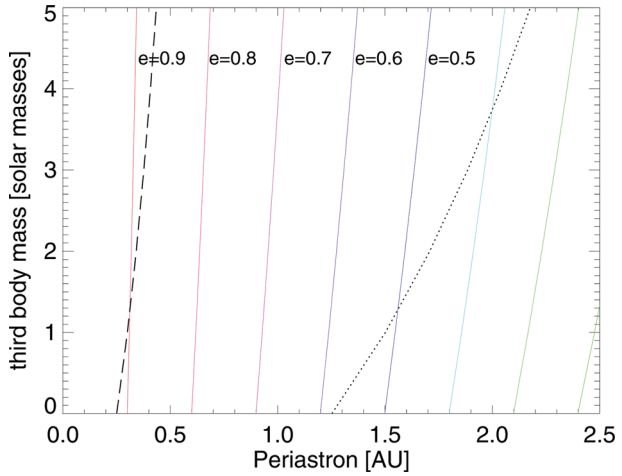

Figure 15. Periastron distance of a body orbiting around the binary star (with a period of 600 d) as a function of its mass. The plot reports this relation at different values of eccentricity. We assume the XRB to be only one heavy body of $M = 10$ M$_\odot$. Considering a prograde motion of the third body, the black dashed line represents the critical distance for a binary separation of 0.1 au and the black dotted line represents the critical distance for a binary separation of 0.5 au. The calculation of the critical distances has been performed following equation (1) of Donnison & Mikulskis (1995) (see also Harrington 1975, for details).

(i) A limit cycle of accretion disc ionization instability should produce periodical outbursts, as in the case of dwarf novae (e.g. Cannizzo 1993; Janiuk & Czerny 2011). Concerning this hypothesis, the duration and the recurrence period of the 4U 1630–472 outbursts seem to be plausible for a limit cycle (Lasota 2001). However, their time profile is not always the one expected for a limit cycle, 'fast rise and exponential decay' (FRED; Lasota 2001). As reported by, for example, Janiuk & Czerny (2011), other factors such as the accretion rate from the companion star could superimpose other outbursts to those produced by the limit cycle in analogy with the case of dwarf novae super-outbursts (e.g. the 2002–2004 outburst). Nevertheless, as Parmar et al. (1995) noticed, it is unlikely that the instability could maintain the phase for more than 40 yr, while this phenomena seems to be more plausible in the case of H 1743–322 (e.g. Capitanio et al. 2010), which usually shows three or four outbursts with the same period and then the next few outbursts show a different period.

(ii) Another hypothesis could be the presence of a third body orbiting around the binary system in a hierarchical configuration (Parmar et al. 1995), that is, a body moving on an approximately Keplerian orbit around the barycentre of the binary system. Fig. 15 represents the derived relation, given by the Kepler laws, between the periastron distance of a body, orbiting around a binary, with a 600-d period, as a function of its mass. We roughly consider the binary system as only one heavy body of 10 M$_\odot$ consistent with the result reported by Seifina et al. (2014). We perform this calculation for different eccentricity values of the orbit, finding that, for a highly eccentric orbit ($e > 0.7$), this third body could reach a distance lower than an astronomical unit (au) and its mass could even be very high. However, the three-body orbital stability criteria (see Donnison & Mikulskis 1995, and references therein) imply that the binary remains stable against the perturbation of the third body if it is at a distance larger than a critical distance (Harrington 1975; Donnison & Mikulskis 1995). This distance strongly depends on the separation between the components of the binary system. As reported by Augusteijn et al. (2001), the IR properties of 4U 1630–472 are similar to those of other BHCs, such as GROJ1655–40 or SAXJ1819.3–2525, that host a relatively early-type secondary companion. Thus, the distance between the companion star and the BH could be roughly 0.1 au (e.g. Remillard & McClintock 2006). The black dashed line in Fig. 15 shows critical periastron distance as a function of the third-body mass for a binary system separation of 0.1 au and a prograde motion of the third body following equation (1) of Donnison & Mikulskis (1995) and the results reported by Harrington (1975).[3] This calculation strongly depends on the binary separation, which for 4U 1630–472 is substantially unknown. For example, the black dotted line in Fig. 15 represents the critical distance as a function of the third-body mass in the case of a binary separation of 0.5 au. A hierarchical eccentric three-body system near the instability limit could be a good candidate to cause periodical outbursts. In fact, in this case, the presence of the third body perturbs the central binary system, and when it reaches the periastron, its vicinity could induce the instabilities in the accretion disc, triggering an outburst. Because there are too many unknown parameters, it is difficult to determine if the sporadic increase of the recurrence period is compatible with an orbit perturbation of the triple system. Nevertheless, it is possible to hypothesize that the perturbation of the orbital period could be due to an effect such as the Kozai effect, a periodic exchange between the orbit inclination and the orbit eccentricity of the third body (Kozai 1962). Thus, the diagram in Fig. 15 should be considered as a first approximation of the problem. In fact, we did not take into account the relativistic effects and the fact that the mass of the third body could also be comparable with the other two. In this case, the dynamics of a three-body system containing three comparable masses remains a major unsolved problem (Donnison & Mikulskis 1992). However, 4U 1630–472 is not the first triple system containing an accreting binary. For example, there are several millisecond pulsars that belong to a hierarchical three-body system, such as B1620–26, a millisecond pulsar with a white dwarf and a planetary-mass object (Thorsett et al. 1999), or the recently published PSR J0337+1715, containing a millisecond pulsar and two other stars in a hierarchical configuration (Ramson et al. 2014). The presence of a third body in this kind of system is easy to detect and to study because of the typical time delay of the spin period of the pulsars (see Ramson et al. 2014, and references therein).

(iii) We could also suppose a system with a high eccentric orbit of the companion star. However, this should imply a massive companion star (Parmar et al. 1995) in a high-mass X-ray binary (HMXRB) system. Even though the IR data cannot exclude the Be nature of the system, the spectral behaviour, the duration of the outbursts and the signature of the presence of a BH as a compact object (Seifina et al. 2014) make this hypothesis unlikely. In fact, the first case of a Be HMXRB hosting a BH has recently been reported in the literature (Munar-Adrover et al. 2014). This source shows a spectral behaviour totally different from the behaviour of 4U 1630–472.

(iv) We could consider a LMXRB in a wide eccentric orbit, which is unacceptable from an evolutionary point of view. In fact, LMXRBs are old systems with circular orbits of periods that spans from a few hours (ultra-compact sources) to some days. Because of the huge orbital period (600–700 d), even a subsequent capture of the companion star or a modification of its orbit due to interactions with other bodies are not consistent with the Roche lobe

[3] The critical distance for retrograde motion is quite similar to that for prograde motion and is omitted for clarity

overflow phenomenon. In fact, the companion star of a binary system such as 4U 1630–472 should be very small (Augusteijn et al. 2001) and needs to be very near to the central BH to allow the accretion coming from the Lagrange point ($d \sim 0.1$ au Remillard & McClintock 2006). Thus, considering the Keplerian orbits in Fig. 15 as the possible orbits of an object captured by a 10-$M_{\odot}$ BH, such a small periastron distance could be reached only with a degenerate eccentricity of the orbit.

(v) Also, the constant refilling from the companion star, as reported by Trudolyubov et al. (2001), is unlikely. In fact, even accepting that a constant refilling of the outer disc could cause the periodical outbursts, this implies a constant quantity of accreted matter, which in some way reaches, after about 600 d, a critical mass that, in turn, triggers the outburst, involving always the same quantity of matter. Thus, the outbursts should always have the same luminosity. As Fig. 1 shows, this is not the case of 4U 1630–472.

5 CONCLUSIONS

(i) The 2006 and 2008 outbursts exhibit an unusual behaviour: they do not show any hard emission up to 30 keV throughout the outburst. Probably, the electron corona is quickly thermalized or it has not enough time to heat up. Moreover, at least in the 2006 case, the lack of any radio detection immediately after the enhancement of the ASM flux indicates that the LHS–HSS transition occurred very sharply or did not occur at all. This is quite a rare behaviour for a LMXRB. In fact, outbursts that never reach a soft state (so-called 'failed outbursts') have often been reported in the literature (e.g. Capitanio et al. 2009; Ferrigno et al. 2012, and references therein). On the contrary, 'soft' outbursts are unusual since the launch of X-ray satellites hosting telescopes suitable for hard X-ray emission measurements above 20 keV, such as *BeppoSAX*/phoswich detection system, *RXTE*/HEXTE, *INTEGRAL*/IBIS and *Swift*/BAT.

(ii) The 2010 outburst seems, in contrast, to be a standard outburst, from a high-energy emission point of view. In fact, the source is bright above 30 keV for most of the outburst, although in this case also, as reported by Tomsick et al. (2014), the outburst shows an unusual delay of the final transition to the hard state. Furthermore, the lack of radio emission in the rising phase of the outburst indicates a sharp LHS–HSS transition.

(iii) The 2006 and 2008 outbursts of 4U 1630–472 do not seem to follow the empirical relations found by Wu et al. (2010), Yu et al. (2007) and Yu & Yan (2009) between the hard X-ray luminosity peak of the HS–HSS transition and the subsequent HSS luminosity peak, or the outburst waiting time. These empirical relations imply that the two accretion flows (disc and corona) should be related. Our results give an indication that, at least in these cases, the two accretion flows could be uncorrelated.

(iv) We argue that an important role in the anomalous behaviour of 4U 1630–472 could be played by the periodical outbursts, whatever their origin. The periodicity could be an extra perturbation that is added to the disc instability due to the companion star mass transfer. The interference between these two phenomena could explain, for example, the long and bright outburst occurring between 2002 and 2004.

(v) As we have illustrated in Section 4.3, there are two most plausible explanations for the outbursts being equally spaced in time. The first is the presence of a third body orbiting around the binary system, and the second is the presence of a limit cycle of the accretion disc ionization instability. Concerning the latter hypothesis, it is unlikely that this limit cycle phase could have lasted for such a long time. Instead, considering the third-body hypothesis, we have discussed the possibility that the recurrence period is compatible with a three-body hierarchical system containing an X-ray binary and a third body that could even be quite heavy and near the critical distance. Nevertheless, these calculations strongly depend on the binary system separation that is actually unknown. At odds with this hypothesis is the sporadic 100-d longer outburst recurrence period, previously noticed by other authors but also present in the last three outbursts of the source. However, our simple calculation does not take into account the effect of the space–time deformation on the third body, due to the BH, and the various classical perturbations that affect a hierarchical three-body system, such as the Kozai effect. In fact, the unknown nature of the binary and of the third body leave too many unknown parameters to permit any more refined calculations.

We can conclude that, even though we have demonstrated that the case of 4U 1630–472 could be peculiar with respect to other BHCs, the origin and evolution of the electron corona is a complex mechanism not only related to the spectral evolution of the accretion disc and still not well understood.

ACKNOWLEDGEMENTS

The authors would like to thank Roberto Ricci and Marcello Giroletti for checking the radio data. RC and the other authors thank T. M. Belloni for his help with the timing analysis software. FC also thanks Carla Maceroni, Agnieszka Janiuk, Massimo Cocchi, Agata Rozanska and Melania Del Santo for useful scientific discussions. Special thanks go to Valeria Mangano for scientific discussions and careful editing of the text. The *RXTE* data were obtained through the High Energy Astrophysics Science Archive Research Center (HEASARC) online service. The *INTEGRAL* data were obtained through the *INTEGRAL* Science Data Center (ISDC) online service. The *Swift*/BAT light curve is part of the *SWIFT*/BAT transient monitor results provided by the *Swift*/BAT team.

REFERENCES

Abe Y., Fukazawa Y., Kubota A., Kasama D., Makishima K., 2005, PASJ, 57, 629
Augusteijn T., Kuulkers E., van Kerkwijk M. H., 2001, A&A, 375, 447
Belloni T., Hasinger G., 1990, A&A, 230, 103
Belloni T., Homan J., Casella P., van der Klis M., Nespoli E., Lewin W. H. G., Miller J. M., Méndez M., 2005, A&A, 440, 207
Calvelo D. E., Fender R. P., Corbel S., Brocksopp C., Tzioumis T., 2010, ATel, 2370
Cannizzo J. K., 1993, ApJ, 419, 318
Capitanio F., Belloni T., del Santo M., Ubertini P., 2009, MNRAS, 398, 1194
Capitanio F., Ubertini P., Tarana A., Del Santo M., Persi P., Roth M., 2010, in Proc. 4th Int. MAXI Workshop: The First Year of MAXI: Monitoring Variable X-ray Sources. p. 129
Corbel S., Tzioumis T., 2008, ATel, 1349
Courvoisier T. J.-L. et al., 2003, A&A, 411, L53
Díaz Trigo M., Miller-Jones J. C. A., Migliari S., Broderick J. W., Tzioumis T., 2013, Nat, 504, 260
Dieters S. et al., 2000, ApJ, 538, 307
Donnison J. R., Mikulskis D. F., 1992, MNRAS, 254, 21
Donnison J. R., Mikulskis D. F., 1995, MNRAS, 272, 1
Dunn R. J. H., Fender R. P., Körding E. G., Belloni T., Cabanac C., 2010, MNRAS, 403, 61
Fabian A., Ross R., 2010, Space Sci. Rev., 157, 167
Fender R., 2006, in Lewin W., van der Klis M., eds, Compact Stellar X-Ray Sources, Cambridge Astrophysics Series, No. 39. Cambridge Univ. Press, Cambridge, p. 381

Fender R. et al., 1999, ApJ, 519, L165
Fender R. P., Belloni T. M., Gallo E., 2004, MNRAS, 355, 1105
Ferrigno C., Bozzo E., Del Santo M., Capitanio F., 2012, A&A, 537, L7
Gallo E., Tomsick J., Fender R., Tzioumis T., Sault R., Maccarone T., Belloni T., 2006, ATel, 685
Gallo E., Miller J., Brendan P., Fender R., 2012, MNRAS, 423, 590
Gehrels N. et al., 2004, ApJ, 611, 1005
Hannikainen D., Sault B., Kuulkers E., Wu K., Jones P., Hunstead R., 2002, ATel, 108
Harrington R. S., 1975, AJ, 80, 1081
Hjellming R. M. et al., 1999, ApJ, 514, 383
Homan J., Belloni T., 2005, Ap&SS, 300, 107
Homan J., Wijands R., van der Klis M., Belloni T., van Paradijs J., Klein-Wolt M., Fender R., Méndez M., 2001, ApJS, 132, 377
Hua X., Titarchuk L., 1995, ApJ, 449, 188
Jahoda K., Markwardt C. B., Radeva Y., Rots A. H., Stark M. J., Swank J. H., Strohmayer T. E., Zhang W., 2006, ApJS, 163, 401
Janiuk A., Czerny B., 2011, MNRAS, 414, 2186
Jourdain E., Gotz D., Westergaard N. J., Natalucci L., Roques J. P., 2008, in Proc. 7th INTEGRAL Workshop, PoS(Integral08)144
Kalemci E., Tomsick J. A., Yamaoka K., Ueda Y., 2008, ATel, 1348
King A. L. et al., 2014, ApJ, 784, L2
Kozai Y., 1962, AJ, 67, 591
Krimm H. A. et al., 2013, ApJS, 209, 14
Kubota A., Tanaka Y., Makishima K., Ueda Y., Dotani T., Inoue H., Yamaoka K., 1998, PASJ, 50, 667
Kubota A. et al., 2007, PASJ, 59, 185
Kuulkers E., Parmar A. N., Kitamoto S., Cominsky R. L., Sood R. K., 1997, MNRAS, 291, 81
Kuulkers E., Wijnands R., Belloni T., Méndez M., van der Klis M., van Paradijs J., 1998, ApJ, 494, 753
Lasota J.-P., 2001, New Astron. Rev., 45, 449
Laurent P., Titarchuk L., 2007, ApJ, 656, 1056
Leahy D. A., Darbro W., Elsner R. F., Weisscopf M. C., Kahn S., Sutherland P. G., Grindlay J. E., 1983, ApJ, 266, 160
Lebrun F. et al., 2003, A&A, 411, 141
Maccarone T., 2003, A&A, 409, 697
Magdziarz P., Zdziarski A. A., 1995, MNRAS, 273, 837
Malzac J., Belmont R., 2009, MNRAS, 392, 570
Miyakawa T., Yamaoka K., Homan J., Saito K., Ditani T., Yoshida A., Inoue H., 2008, PASJ, 60, 637
Miyamoto S., Kimura K., Kitamoto S., Dotani T., Ebisawa K., 1991, ApJ, 383, 784
Munar-Adrover P., Paredes J. M., Ribó M., Iwasawa K., Zabalza V., Casares J., 2014, ApJ, 786, 11
Muñoz-Darias T., Motta S., Belloni T. M., 2011, MNRAS, 410, 679
Neilsen J., Coiriat M., Fender R., Lee G. C., Ponti G., Tzioumis T., Edwards P., Broderick J. W., 2014, ApJ, 784, L5
Parmar A. N., Angelini L., White N. E., 1995, ApJ, 452, L29
Petrucci P. O et al., 2001, ApJ, 556, 716
Ponti G., Fender R. P., Begelman M. C., 2012, MNRAS, 422, L11
Poutanen J., Svensson R., 1996, ApJ, 470, 249
Priedhorsky W. C., 1986, Ap&SS, 126, 89
Ramson S. M. et al., 2014, Nat, 505, 520
Remillard R. A., McClintock J. E., 2006, ARA&A, 44, 49
Rodriguez J. et al., 2006, MNRAS, 366, 274
Ross R. R., Fabian A. C., 2007, MNRAS, 381, 1697
Russell D. M., Miller-Jones J. C. A., Maccarone T. J., Yang Y. J., Fender R. P., Lewis F., 2011, ApJ, 739, L19
Sakura N., Sunyaev R. A., 1973, A&A, 24, 337
Seifina E., Titarchuk L., Shaposhnikov N., 2014, ApJ, 789, 57
Shaposhnikov N., Titarchuk L., 2009, ApJ, 699, 453
Thorsett S. E., Arzoumanian Z., Camilo F., Lyne A. G., 1999, ApJ, 523, 763
Titarchuk L., 1994, ApJ, 434, 570
Tomida H. et al., 2009, ATel, 2363
Tomsick J. A., 2005, ATel, 675
Tomsick J., Lapshov I., Kaaret P., 1998, ApJ, 494, 747
Tomsick J., Corbel S., Goldwrum A., Kaaret P., 2005, ApJ, 630, 413
Tomsick J. A., Shaposhnikov N., Swank J. H., 2009, ATel, 2365
Tomsick J. A., Yamaoka K., Corbel S., Kalemci E., Migliari S., Kaaret P., 2014, ApJ, 791, 70
Trudolyubov S. P., Borozdin K. N., Priedhorsky W. C., 2001, MNRAS, 322, 309
Ubertini P. et al., 2003, A&A, 411, L131
Wilms J., NowakM. A., Pottschmidt K., Pooley G. G., Fritz S., 2006, A&A, 447, 245
Wu Y. X., Yu W., Yan Z., Sun L., Li T. P., 2010, A&A, 512, A32
Yu W., Yan Z., 2009, ApJ, 701, 1940
Yu W., Lamb F. K., Fender R., van der Klis M., 2007, ApJ, 663, 1309
Zdziarski A. A., Gierlinski M., 2004, Progress of Theoretical Physics Supplement, 155, 99
Zdziarski A. A., Johnson W. N., Magdziarz P., 1996, MNRAS, 283, 193
Zhang W., Jahoda K., Swank J. H., Morgan E. H., Giles A. B., 1995, ApJ, 449, 930

This paper has been typeset from a TEX/LATEX file prepared by the author.